

Absolute negative mobility induced by white Poissonian noise

Jakub Spiechowicz, Jerzy Łuczka, Peter Hänggi

Angaben zur Veröffentlichung / Publication details:

Spiechowicz, Jakub, Jerzy Łuczka, and Peter Hänggi. 2013. "Absolute negative mobility induced by white Poissonian noise." *Journal of Statistical Mechanics: Theory and Experiment* 2013 (02): P02044. <https://doi.org/10.1088/1742-5468/2013/02/p02044>.



Absolute negative mobility induced by white Poissonian noise

J Spiechowicz¹, J Łuczka¹ and P Hänggi²

¹ Institute of Physics, University of Silesia, 40-007 Katowice, Poland

² Institute of Physics, University of Augsburg, D-86135 Augsburg, Germany

E-mail: j.spiechowicz@gmail.com, Jerzy.Luczka@us.edu.pl

and hanggi@physik.uni-augsburg.de

Abstract. We study the transport properties of inertial Brownian particles which move in a *symmetric* periodic potential and are subjected to both a *symmetric*, unbiased time-periodic external force and a biased Poissonian white shot noise (of non-zero average F) which is composed of a random sequence of δ -shaped pulses with random amplitudes. Upon varying the parameters of the white shot noise, one can conveniently manipulate the transport direction and the overall nonlinear response behavior. We find that within tailored parameter regimes the response is *opposite* to the applied average bias F of such white shot noise. This particular transport characteristic thus mimics that of a nonlinear absolute negative mobility (ANM) regime. Moreover, such white shot noise driven ANM is robust with respect to the statistics of the shot noise spikes. Our findings can be checked and corroborated experimentally by the use of a setup that consists of a single resistively and capacitively shunted Josephson junction device.

Contents

1. Introduction	2
2. The model	3
3. Transport properties of a Brownian particle driven by white Gaussian and white Poissonian shot noise	6
3.1. The Ohmic-like transport regime	8
3.2. The regime of absolute negative mobility	9
3.3. Controlling transport.	10
3.4. The robustness of ANM to amplitude statistics	10
3.5. The comparison with deterministic bias	11
4. Conclusions	12
Acknowledgments	13
References	13

1. Introduction

In accordance with the Le Chatelier–Braun principle, when an external deterministic force F acts on a particle with all other forces set to zero on average, the long time, stationary average particle velocity $\langle v \rangle$ is expected to become an increasing function of the load F , at least for small bias values F . For an electrical (electronic) device, the current–voltage characteristics exhibits a similar property: if the voltage V increases, the current I increases as well. The Ohmic characteristic $I = (1/R)V$ presents an example. This behavior is usually characterized as ‘normal transport’ behavior. In contrast, the anomalous transport features are (i) a negative differential mobility or conductivity (meaning that the velocity or current decreases with increasing force or voltage) and (ii) an absolute negative mobility (ANM) or conductivity, i.e. the velocity or current exhibits an opposite sign to the applied force which is starting out at zero force or voltage; i.e. the system response is opposite to the applied force.

Such absolute negative mobility has been experimentally detected in a variety of systems, both classical and quantum. Typical situations and cases where ANM has been detected are p-modulation-doped GaAs quantum wells [1], sequential resonant tunneling semiconductor superlattices that are driven by intense terahertz electric fields [2], relaxing Xe plasma ionized by a hard x-ray pulse [3], sliding charge-density waves at sufficiently low temperatures [4], in microfluidic systems with colloidal beads in an aqueous buffer solution [5], in a three-terminal configuration in a two-dimensional electron gas [6], and the transport of vortices in superconductors with inhomogeneous pinning under a driving force [7] and in Josephson junctions [8]. Rather recently, a coherent absolute negative mobility regime has been observed and described for ac and dc driven ultracold atoms in an optical lattice [9].

Yet further examples of ANM have been described theoretically for the nonlinear response in ac–dc driven tunneling transport [10], the dynamics of cooperative Brownian motors [11], Brownian transport containing a complex topology [12, 13] and some multi-state models with state-dependent noise [14]. The effect of an absolute negative mobility can occur also in driven systems such as those of nonlinear inertial Brownian dynamics [15]–[18], overdamped nonlinear Brownian motion in the presence of time-delayed feedback [19], transport of asymmetric particles in a periodically segmented 2D channel [20] and for a system of two coupled resistively shunted Josephson junctions [21].

The key ingredient for the occurrence of ANM in all those listed cases is that the system (i) is driven far away from thermal equilibrium into a time-dependent nonequilibrium state and the resulting dynamics is such that (ii) it is exhibiting a vanishing, unbiased average nonequilibrium response. In the presence of a finite bias F , the ANM response in a symmetric periodic potential is such that an average, anti-symmetric transport velocity $\langle v(F) \rangle$, obeying $\langle v(F) \rangle = -\langle v(-F) \rangle$, occurs around the zero bias force $F = 0$. This situation must be contrasted with the nonequilibrium transport generated by the ratchet mechanism [22]: there, a non-vanishing transport velocity occurs even for vanishing bias $F = 0$, and thus no anti-symmetric mobility behavior occurs around the zero-bias regime. The reader is thus advised to carefully distinguish between anomalous mobility regimes that are characterized as a negative differential mobility regime, or as an absolute negative mobility regime or as a nonlinear negative-valued mobility away from the zero-bias regime [16].

With this work, we substitute the deterministic static force F by a random force $\eta(t)$ of non-zero average. To allow for the comparison with the case of a deterministic load $F \neq 0$, we require that the mean value of the random force $\eta(t)$ equals the value F . As a model for such a random force we use a random sequence of exponentially distributed δ -shaped pulses with random amplitudes. This constitutes a generalized white Poissonian shot noise process; e.g. see [23] for its detailed statistical properties. We demonstrate that this shot noise can induce ANM and in the regime of ANM, it behaves on average statistically similarly to a deterministic constant bias F . Moreover, the ANM phenomenon is robust with respect to the distribution of the random amplitudes of the δ -pulses.

The layout of the present work is as follows. In section 2 we detail the model of a driven inertial Brownian particle. In section 3 we detail more closely the stochastic force acting on the particle and elucidate the resulting transport properties. The findings are contrasted with those for an equivalent setup consisting of a deterministic bias. section 4 provides our summary and some conclusions.

2. The model

In what follows we consider an ensemble of classical, statistically independent Brownian particles undergoing transport in an effectively one-dimensional geometry. For such a one-dimensional system, the *minimal* model of the classical Brownian particle exhibiting the ANM is formulated in terms of the equation of motion for a particle of mass M (i) moving in a symmetric spatially periodic potential $V(x) = V(x + L)$ of period L , (ii) being driven by an unbiased time-periodic force $A \cos(\Omega t)$ with angular frequency Ω and amplitude strength A , and (iii) exposed to a static force F . All three components are essential in order to take the system away from a thermal equilibrium state into a time-dependent

driven nonequilibrium state such that the limiting Le Chatelier–Braun principle no longer applies. The corresponding Langevin equation reads [15]

$$M\ddot{x} + \Gamma\dot{x} = -V'(x) + A \cos(\Omega t) + F + \sqrt{2\Gamma k_B T} \xi(t). \quad (1)$$

Here, the dot and the prime denote differentiation with respect to time t and the Brownian particle's coordinate x , respectively. The parameter Γ is the friction coefficient, k_B is the Boltzmann constant and T is the temperature. Thermal equilibrium fluctuations are modeled by δ -correlated Gaussian white noise $\xi(t)$ of zero mean and unit intensity, i.e.

$$\langle \xi(t) \rangle = 0, \quad \langle \xi(t)\xi(s) \rangle = \delta(t - s). \quad (2)$$

We are interested in the asymptotic long time regime, where the averaged velocity assumes the periodicity of the driving [24], i.e.,

$$\langle v \rangle = \lim_{t \rightarrow \infty} \frac{\Omega}{2\pi} \int_t^{t+2\pi/\Omega} \langle v(s) \rangle ds, \quad (3)$$

where $\langle v(s) \rangle$ indicates the average over noise realizations (ensemble average). In the deterministic case ($T = 0$), an additional averaging over initial conditions must be performed.

From the symmetry of the Langevin equation it follows that the transformation $F \rightarrow -F$ implies $\langle v \rangle \rightarrow -\langle v \rangle$. In other words, the average velocity $\langle v \rangle(F)$ as a function of the load F fulfills the relation $\langle v \rangle(-F) = -\langle v \rangle(F)$. In particular, it follows that the transport vanishes identically, $\langle v \rangle \equiv 0$, for $F = 0$. This is in clear contrast to the case for a ratchet mechanism which exhibits finite transport at vanishing static bias [22]. Generally, the averaged velocity $\langle v \rangle$ is a nonlinear function of the bias F . However, for small values of F one can expect a linear response regime to be present and $\langle v \rangle$ assumes the form of a linear function of small bias; i.e.,

$$\langle v \rangle = \mu F. \quad (4)$$

In the normal transport regime, the mobility coefficient μ is positive, $\mu > 0$; in distinct contrast, $\mu < 0$ for ANM. In [15], it has been shown that the above system exhibits ANM and there are two fundamentally different mechanisms for ANM: (a) induced by thermal fluctuations and (b) generated by deterministic dynamics.

We now substitute the deterministic static force F by a stochastic force $\eta(t)$. Such a case is important because it could help to explain and clarify the understanding of unusual transport properties not only in physical but also in biological systems, e.g., the bi-directionality of the net cargo transport inside living cells, where there is no systematic deterministic load but rather random collisions in the form of kicks and impulses. Thus, in place of equation (1) we shall consider the setup

$$M\ddot{x} + \Gamma\dot{x} = -V'(x) + A \cos(\Omega t) + \eta(t) + \sqrt{2\Gamma k_B T} \xi(t). \quad (5)$$

The potential $V(x)$ is assumed to be in the simplest *symmetric* form

$$V(x) = \Delta V \sin(2\pi x/L). \quad (6)$$

In order to make the comparison with the case of the deterministic load $F \neq 0$, we set the mean value of the random force $\eta(t)$ equal to F ; i.e. $\langle \eta(t) \rangle = F$. As a model for such a stochastic biased forcing we propose a random sequence of δ -shaped pulses with random

amplitudes defined in terms of generalized white Poissonian shot noise [23, 25]:

$$\eta(t) = \sum_{i=1}^{n(t)} z_i \delta(t - t_i), \quad (7)$$

where the t_i are the arrival times of a Poissonian counting process $n(t)$ with parameter λ . Put differently, the probability for occurrence of k impulses in the time interval $[0, t]$ is governed by the Poisson distribution; i.e.,

$$\Pr\{n(t) = k\} = \frac{(\lambda t)^k}{k!} e^{-\lambda t}. \quad (8)$$

Likewise, the interval s between successive Poisson arrival times $s = t_i - t_{i-1}$ is exponentially distributed with the probability density $\lambda \exp(-\lambda s)$. The parameter λ determines the mean number of δ -pulses per unit time or equivalently the mean spiking rate of the δ -pulses. The amplitudes $\{z_i\}$ of the δ -pulses denote independent random variables. These amplitudes are statistically distributed according to a common probability density $\rho(z)$. The process $\eta(t)$ presents white noise of finite mean and a covariance given by

$$\langle \eta(t) \rangle = \lambda \langle z_i \rangle, \quad \langle \eta(t)\eta(s) \rangle - \langle \eta(t) \rangle \langle \eta(s) \rangle = 2D_P \delta(t - s), \quad (9)$$

where $\langle z_i \rangle$ is an average over the amplitude distribution $\rho(z)$. Poissonian white noise is statistically symmetric if the density $\rho(z)$ is symmetric, i.e. when $\rho(z) = \rho(-z)$. Consequently, $\langle \eta(t) \rangle = 0$. However, we shall not consider unbiased driving but instead consider biased white Poissonian noise for which $\langle \eta(t) \rangle \neq 0$. The white Poissonian noise intensity D_P reads

$$D_P = \frac{\lambda \langle z_i^2 \rangle}{2}. \quad (10)$$

We further assume that thermal equilibrium noise $\xi(t)$ is uncorrelated with nonequilibrium noise $\eta(t)$, so $\langle \xi(t)\eta(s) \rangle = \langle \xi(t) \rangle \langle \eta(s) \rangle = 0$.

Next we use a dimensionless form of equation (5). This can be achieved in several ways. Here we propose the use of the period L as a length scale and for time the scale $\tau = L\sqrt{M/\Delta V}$ [26]. Consequently, equation (5) can be rewritten in a dimensionless form as

$$\ddot{\hat{x}} + \gamma \dot{\hat{x}} = -\hat{V}'(\hat{x}) + a \cos(\omega \hat{t}) + \hat{\eta}(\hat{t}) + \sqrt{2\gamma D_G} \hat{\xi}(\hat{t}), \quad (11)$$

where $\hat{x} = x/L$ and $\hat{t} = t/\tau$. Other rescaled dimensionless parameters are the friction coefficient $\gamma = \tau\Gamma/M$, the amplitude $a = LA/\Delta V$ and the angular frequency $\omega = \tau\Omega$ of the time-periodic driving. The rescaled potential $\hat{V}(\hat{x}) = V(L\hat{x})/\Delta V = \sin(2\pi\hat{x})$ possesses the unit period: $\hat{V}(\hat{x}) = \hat{V}(\hat{x}+1)$. We introduced the dimensionless thermal noise intensity $D_G = k_B T/\Delta V$, so the Gaussian white noise of vanishing mean $\hat{\xi}(\hat{t})$ possesses the auto-correlation function $\langle \hat{\xi}(\hat{t})\hat{\xi}(\hat{s}) \rangle = \delta(\hat{t}-\hat{s})$. Similarly, the rescaled Poissonian white shot noise is δ -correlated as well; i.e., $\langle \hat{\eta}(\hat{t})\hat{\eta}(\hat{s}) \rangle - \langle \hat{\eta}(\hat{t}) \rangle \langle \hat{\eta}(\hat{s}) \rangle = 2\hat{D}_P \delta(\hat{t} - \hat{s})$, with $\hat{D}_P = \hat{\lambda} \langle \hat{z}_i^2 \rangle / 2$, where $\hat{\lambda} = \tau\lambda$ and $\hat{z}_i = z_i/\sqrt{M\Delta V}$. Hereafter, we will use only dimensionless variables and shall omit the ‘hat’ notation in all quantities appearing in equation (11).

The deterministic dynamics corresponding to equation (11) exhibits an extremely rich and complex behavior. Depending on the parameter values, periodic, quasiperiodic and

chaotic motion can be observed [27]. In some regimes, ergodicity is broken and the direction of the spontaneous transport depends on the choice for the initial conditions. Different initial conditions of position and velocity may lead to radically different asymptotic behavior; i.e. various attractors may coexist. The asymptotic regime can be classified as either being a locked or a running state. The regime of the running state is the crucial ingredient for the occurrence of non-vanishing transport in the deterministic regime, allowing the system to explore all of space. At non-zero temperature, the system will be typically ergodic with thermal fluctuations enabling diffusive transport with stochastic escape events connecting coexisting deterministic disjoint attractors [28]. In particular, transitions between neighboring locked states give rise to diffusive directed transport.

There exist a wealth of physical systems that can be described by using equations of the form in equation (11). An important case that comes to mind is that of the semi-classical dynamics of a phase difference across a resistively and capacitively shunted Josephson junction which is driven by both a time-periodic and a random force [29]. For this setup the space coordinate of the Brownian particle x and the driving force correspond to the phase difference and the current applied to the Josephson junction, respectively. Other specific systems are rotating dipoles in external fields [30], superionic conductors [31] and charge-density waves [32], to name but a few.

3. Transport properties of a Brownian particle driven by white Gaussian and white Poissonian shot noise

The Fokker–Planck–Kolmogorov–Feller master equation corresponding to the Langevin equation (11) (cf. [25]) cannot be studied using closed analytical forms. Consequently, we have to resort to comprehensive numerical simulations of the white Gaussian and white shot noise driven Langevin dynamics. Details of the numerical scheme employed can be found in [33, 34]. We have chosen the time step to be $0.002 \times 2\pi/\omega$ and used initial conditions $\{x(0), \dot{x}(0)\}$ that are equally distributed over the interval $[0, 1]$ and $[-2, 2]$, respectively (remember that the rescaled potential possesses the unit period). Noise averaging has been performed over 10^3 – 10^6 different stochastic realizations and, additionally, over one period of the external driving period $2\pi/\omega$. All numerical calculations have been done by use of a CUDA environment implemented on a modern desktop GPU. This scheme allowed for a speed-up of a factor of the order ~ 100 times as compared to a common present-day CPU method [35].

To gain insight into the role of the white Poissonian shot noise we first examine the influence of the noise parameters λ and D_P on the characteristics of the stochastic realizations. To be definite, we assume that the amplitudes $\{z_i\}$ of the δ -kicks are exponentially distributed with the probability density

$$\rho_1(z) = \zeta^{-1}\theta(z)e^{-z/\zeta}, \quad (12)$$

where $\theta(z)$ denotes the Heaviside step function; i.e. the noise amplitudes take on only positive values, $z_i > 0$. According to equation (12), the statistical moments of these amplitudes $\{z_i\}$ are given by

$$\langle z_i^k \rangle = k!\zeta^k, \quad k = 1, 2, 3, \dots \quad (13)$$

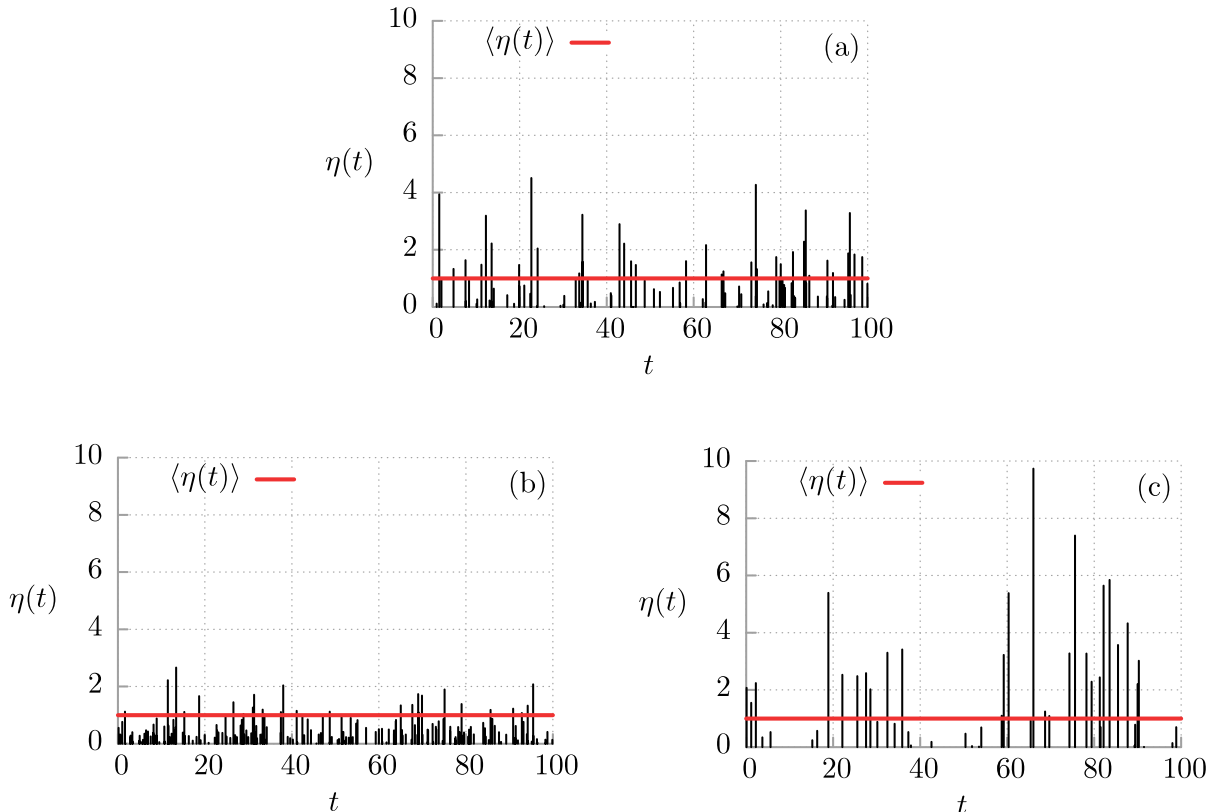


Figure 1. Three illustrative realizations of Poissonian white shot noise $\eta(t)$. The amplitudes $\{z_i\}$ of the δ -spikes are distributed according to the exponential probability density (12). In all three cases, the mean value is held fixed, i.e., $\langle\eta(t)\rangle = \zeta\lambda = \sqrt{\lambda D_P} = 1$. The spike rate λ and the noise intensity D_P are varied as follows: in (a): $\lambda = 1$, $D_P = 1$; in (b): $\lambda = 2$, $D_P = 0.5$; in (c): $\lambda = 0.5$, $D_P = 2$.

From equations (9) and (10) it follows that the mean value $\langle\eta(t)\rangle$ and the intensity D_P of the white shot noise read

$$\langle\eta(t)\rangle = \lambda\zeta, \quad D_P = \lambda\zeta^2. \quad (14)$$

We next use λ and D_P as the quantifiers for transport; this yields $\langle\eta(t)\rangle = \sqrt{\lambda D_P}$ and $\zeta = \sqrt{D_P/\lambda}$. Three typical realizations of white Poissonian noises are depicted in figure 1. In figure 1(a), the mean spiking rate of pulses λ and the noise intensity D_P are fixed at 1. In order to ensure that the condition $\langle\eta(t)\rangle = 1$ holds, we may proceed in two different ways. In the first approach we increase the spiking rate λ while correspondingly reducing the noise intensity D_P . Then the particle is *frequently* kicked by *weak* δ -pulses. This case is depicted in figure 1(b). In the second approach we decrease the spiking rate λ and increase the noise intensity D_P . Then the particle is *rarely* kicked by *large* amplitudes of the δ -spikes; cf. figure 1(c). It is worth mentioning that in the limit of vanishing amplitudes z_i , when $\zeta \rightarrow 0$, and for a divergent spiking rate $\lambda \rightarrow \infty$, with $\lambda\zeta^2 = D_P$ held fixed, the zero-mean process $\eta(t) - \langle\eta(t)\rangle$ approaches Gaussian white noise of intensity D_P .

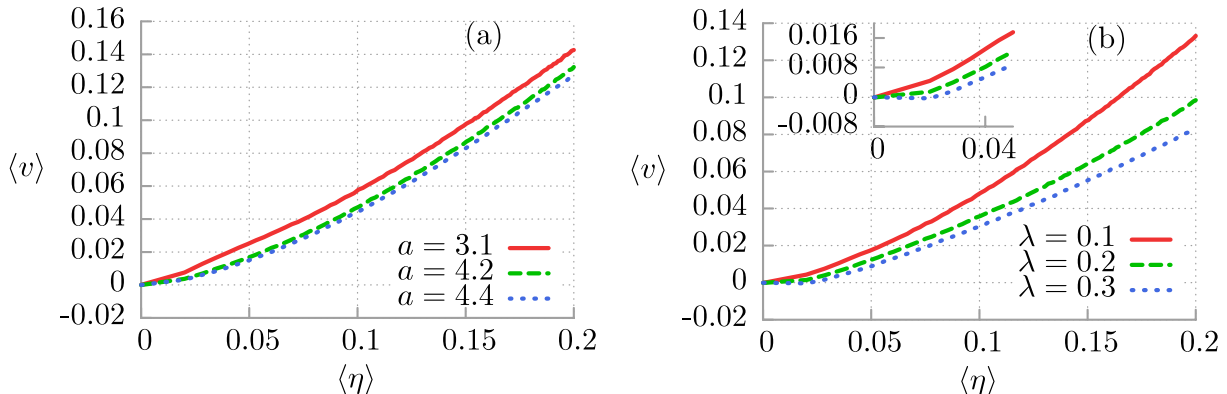


Figure 2. Ohmic-like dependence of the asymptotic, time-averaged asymptotic velocity $\langle v \rangle$ on the mean value of the shot noise $\langle \eta(t) \rangle$. Panel (a): the influence of the amplitude strength a of the time-periodic driving is illustrated for fixed spiking rate $\lambda = 0.1$ of the δ -spikes. Panel (b): the role of the spiking rate is depicted for the ac driving amplitude $a = 4.2$. The spike amplitudes $\{z_i\}$ of the δ -kicks are distributed according to the exponential probability density $\rho_1(z)$ in equation (12). The remaining parameters are fixed as follows: the friction coefficient is $\gamma = 0.9$, the thermal fluctuation intensity is $D_G = 0.001$ and the angular driving frequency is $\omega = 4.9$.

3.1. The Ohmic-like transport regime

Let us comment first on the long time behavior of the driven system considered in equation (11). If the Poissonian white shot noise is absent in equation (11), then the average velocity $\langle v \rangle$ vanishes identically. This feature follows from the presence of reflection symmetry of the potential $V(x)$ and the time reversal symmetry of harmonic driving. Put differently, a directed ratchet transport [22] is absent.

In the presence of white Poissonian shot noise driving, however, a statistical bias emerges [36], which is due to the non-vanishing average. This causes a non-zero mean velocity, which typically assumes the sign of the average of the white shot noise. We recall that there are only *positive* δ -kicks and therefore we expect the average velocity to be positive as well. An opposite behavior would be counterintuitive. Because the dynamics as determined by equation (11) is strongly nonlinear and the stochastic phase space of the system is multidimensional, it should not come as a surprise that the dependence of the average velocity on $\langle \eta(t) \rangle$ is nonlinear as well and may even behave in the non-monotonic manner of the system parameters. The normal expected behavior for the ensemble-averaged and time-averaged velocity is that of an increasing function for $\langle \eta(t) \rangle$. Such a normal regime is depicted in figure 2. We used therein the following parameter values: the friction coefficient has been chosen as $\gamma = 0.9$, the thermal fluctuation intensity is $D_G = 0.001$, and the angular driving frequency is $\omega = 4.9$. In panel (a), the influence of the driving amplitude a is shown. Panel (b) depicts the role of the spiking rate λ of the δ -pulses. The corresponding shot noise characteristics corresponds to rare but large δ -spikes. As a consequence, the average velocity varies almost linearly with the mean value of the shot noise $\langle \eta(t) \rangle$, resulting in an Ohmic-like transport behavior.

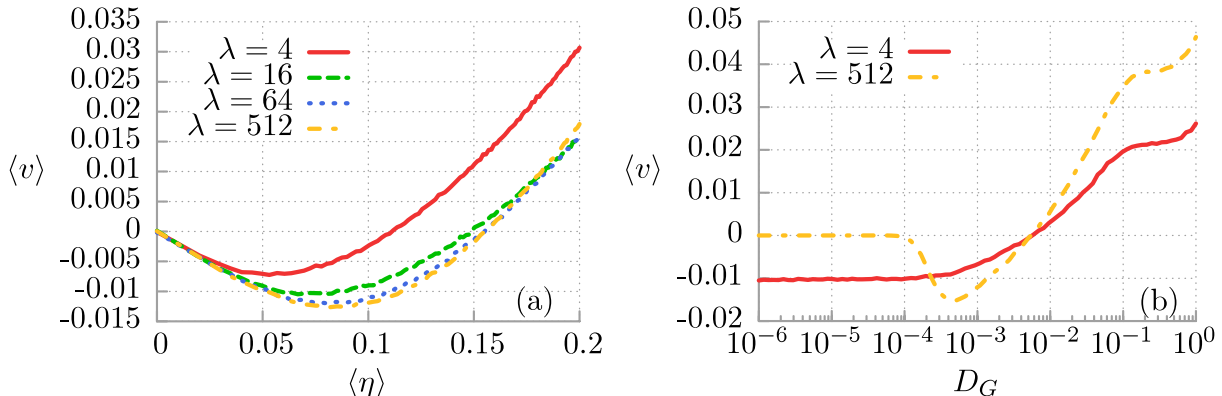


Figure 3. Absolute negative mobility (ANM). Panel (a): the asymptotic time-averaged velocity $\langle v \rangle$ as a function of the mean value of the white shot noise $\langle \eta(t) \rangle$ for various spiking frequencies λ and fixed thermal fluctuation intensity $D_G = 0.001$. In panel (b) the role of the thermal fluctuations is shown for two spiking frequencies $\lambda = 4$ (solid line, $D_P = 6 \times 10^{-4}$) and $\lambda = 512$ (dotted line, $D_P = 2 \times 10^{-5}$). Note that for the value $\lambda = 512$, ANM is induced by thermal fluctuations. There occurs an optimal temperature D_G at which ANM is most pronounced. In both panels: the amplitudes $\{z_i\}$ of the δ -spikes are exponentially distributed; the friction coefficient is $\gamma = 0.9$, and the ac driving amplitude is $a = 4.2$ with an angular driving frequency $\omega = 4.9$.

3.2. The regime of absolute negative mobility

We have randomly searched the parameter space and found that the normal, Ohmic-like transport regime dominates in the parameter space. Keeping in mind that there are only positive δ -kicks of white shot noise acting on the Brownian particle, we inquire whether we can identify parameter regimes for which the stationary mean velocity of the particle assumes negative values, i.e. the particle moves on average oppositely to the applied δ -spikes. In figure 3(a) we exemplify this situation. The characteristic feature is the emergence of extended regimes, $\langle \eta(t) \rangle > 0$, where the average velocity $\langle v \rangle$, starting out from zero, assumes a *negative* response; i.e. ANM occurs. Moreover, there exists an optimal strength for $\langle \eta(t) \rangle$ at which the average velocity assumes its minimal value. We detect that if the spiking rate λ increases, then the minimum of the resulting average transport velocity is lowered. Notably, we have found that there exists a limiting minimal value for the transport velocity which is assumed for $\lambda \rightarrow \infty$. For $\lambda > 512$ (see the dotted line) the velocity characteristics becomes numerically indistinguishable.

The role of thermal fluctuations is depicted in panel (b). Two distinct mechanisms for the ANM-like effect can be observed. For $\lambda = 4$, the negative velocity is caused by deterministic chaotic dynamics because even at zero temperature, $D_G = 0$, the velocity is negative. In this regime, temperature plays a destructive role for ANM: increase of temperature monotonically diminishes the negative average velocity. For $\lambda = 512$, the negative velocity is solely induced by thermal fluctuations. For low temperatures (small D_G) ANM does not occur. If thermal fluctuations grow (D_G increases) the ANM effect emerges and intensifies up to the optimal temperature where ANM is most pronounced. Subsequent increase of the temperature reduces ANM and finally temperature destroys it

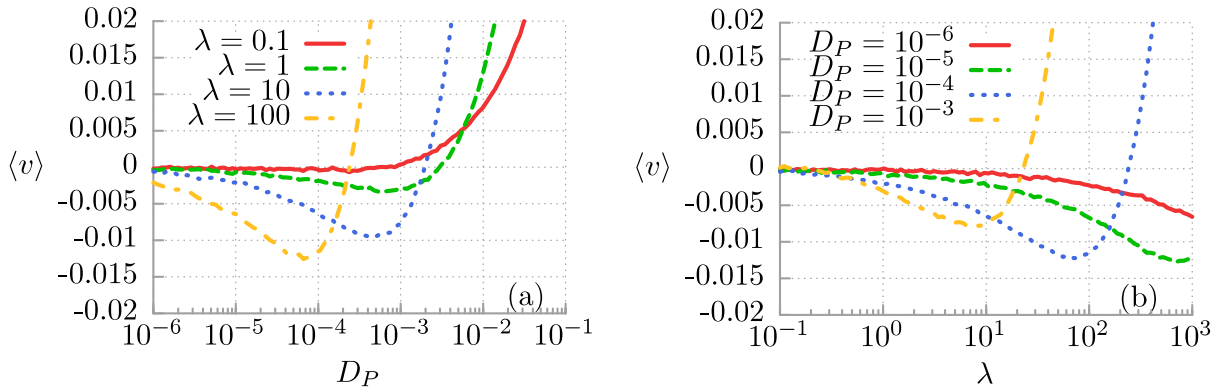


Figure 4. Panel (a): the time-averaged asymptotic velocity $\langle v \rangle$ as a function of the white shot noise intensity D_P for selected values of the spiking frequencies λ . Panel (b): average velocity as a function of the spiking rate λ for several values of the white shot noise intensity D_P . The amplitudes $\{z_i\}$ of the δ -kicks are generated according to the distribution $\rho_1(z)$ and the thermal fluctuation intensity $D_G = 0.001$. Other parameters are the same as those detailed in figure 3.

completely. For ‘high’ temperature, transport is normal. The reader may find a detailed explanation of the origin of anomalous transport in such systems in [15].

3.3. Controlling transport

The transport properties of the Brownian particle can be controlled by varying the parameters of the white Poissonian noise; i.e., the values for λ or D_P . The dependence of the asymptotic average velocity $\langle v \rangle$ on these white shot noise parameters is presented in figures 4(a) and (b). In figure 4(a) we study the role of an increasing white shot noise intensity D_P . As an example, consider the case with $\lambda = 10$ in figure 4(a). For weak shot noise intensity D_P the velocity exhibits ANM and its minimal value decreases with increasing D_P . For strong white shot noise, however, when the intensity D_P is sufficiently large, the average transport velocity turns around towards a normal regime, undergoing a current reversal at some finite noise strength D_P .

The spiking rate λ of the white shot noise also serves as a control parameter for ANM. The numerical findings are depicted in figure 4(b) for a set of selected values of the white shot noise intensity D_P . As before we find that the ANM can be controlled upon varying the spiking rate λ . Again we detect a current reversal at finite spiking rate λ ; this reversal value shifts to much larger spiking frequencies with decreasing white shot noise intensity D_P . In summary, one can conveniently manipulate the direction of the particle transport and tune the ANM regime upon varying the two shot noise parameters.

3.4. The robustness of ANM to amplitude statistics

We also address the dependence of ANM transport for different statistics of the amplitude $\{z_i\}$ entering the generalized white shot noise. In doing so we choose two additional amplitude statistics that derive from special cases of the Gamma distribution. In

particular, we study

$$\rho_2(z) = \zeta^{-2}\theta(z)ze^{-z/\zeta} \quad (15)$$

and

$$\rho_3(z) = \frac{1}{2}\zeta^{-3}\theta(z)z^2e^{-z/\zeta}, \quad (16)$$

where $\theta(z)$ is the Heaviside function. For the density $\rho_2(z)$, the first two moments read

$$\langle z_i \rangle = 2\zeta, \quad \langle z_i^2 \rangle = 6\zeta^2. \quad (17)$$

As a result, upon inspecting equations (9) and (10), we see that the mean value is $\langle \eta(t) \rangle = 2\sqrt{D_P\lambda/3}$ and the white shot intensity reads $D_P = 3\lambda\zeta^2$. Likewise, for the density $\rho_3(z)$, we obtain

$$\langle z_i \rangle = 3\zeta, \quad \langle z_i^2 \rangle = 12\zeta^2. \quad (18)$$

In this case we find that $\langle \eta(t) \rangle = \sqrt{3D_P\lambda/2}$ and $D_P = 6\lambda\zeta^2$. The main difference between the exponential probability density $\rho_1(z)$ in equation (12) and these two integrable densities is a non-monotonic, bell-shaped form; see figure 5(a). As a consequence, with $\rho_1(z)$, very small noise amplitudes are the most likely. In the case of $\rho_2(z)$, the maximum of the density occurs for the amplitudes $z_i = \zeta$, while for $\rho_3(z)$, the amplitudes $z_i = 2\zeta$ are most probable. All three probability densities are depicted in figure 5(a). Panel (b) of this figure depicts the dependence of the averaged velocity $\langle v \rangle$ on the three statistical densities for shot noise amplitudes $\{z_i\}$ at a fixed spiking rate $\lambda = 10$.

We observe that in the regime of ANM, white Poissonian noise with amplitude density $\rho_3(z)$ is slightly more effective. In figure 5(c) we show the behavior for the various amplitude statistics when the spiking rate λ is varied. Overall we find (for the chosen set of three examples) a weak dependence of the ANM regime on the statistics for the noise amplitudes. We therefore may assume that the statistics of the amplitudes only weakly impacts the overall ANM regime, apart from possibly for some cases with abnormal, stylized density features.

3.5. The comparison with deterministic bias

As a final point of analysis, we compare ANM generated by Poissonian shot noise and the external force F which is constant in space and time. So, we have to consider the dimensionless form of the Langevin equation corresponding to (1), namely,

$$\ddot{x} + \gamma\dot{x} = -V'(x) + a\cos(\omega t) + f + \sqrt{2\gamma D_G}\xi(t), \quad (19)$$

where the dimensionless deterministic constant force $f = (L/\Delta V)F$. In order to compare the scenario of the deterministic force f with the system driven by Poissonian white shot noise, we need to impose the additional condition

$$\langle \eta(t) \rangle = f. \quad (20)$$

We consider the following parameter regime: the friction coefficient is $\gamma = 0.9$, the ac driving amplitude is $a = 4.2$, the angular driving frequency is $\omega = 4.9$ and the thermal fluctuation intensity is $D_G = 0.001$. We stress that it is the same parameter regime as in figure 2(b), where the Ohmic-like transport is observed for the case of a low spiking rate $\lambda \leq 0.3$. In figure 6, we show the dependence of the asymptotic average velocity $\langle v \rangle$ on the

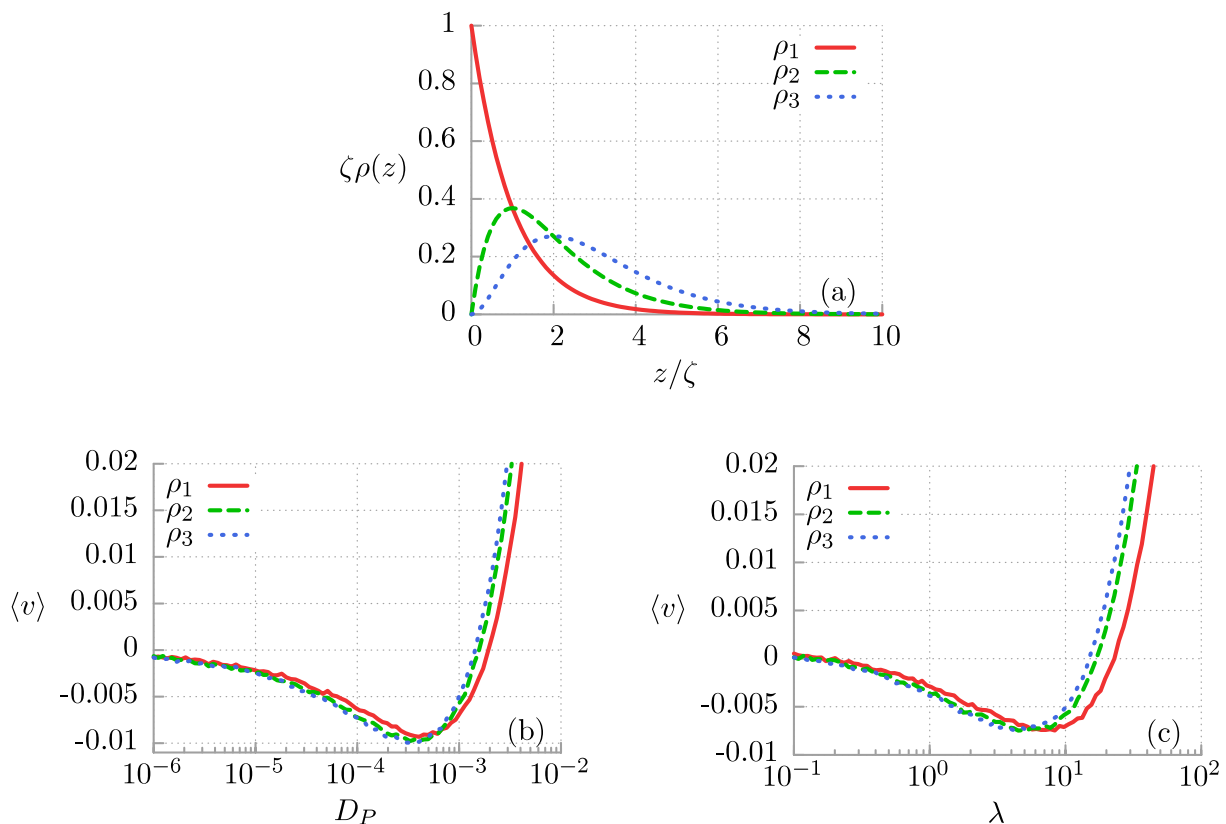


Figure 5. Panel (a): plots of three probability densities of the amplitudes $\{z_i\}$. Panel (b): the dependence of the time-averaged, asymptotic velocity $\langle v \rangle$ on the intensity D_P of the shot noise $\eta(t)$ for three statistical distributions of the amplitudes $\{z_i\}$ of the δ -pulses and for $\lambda = 10$. Panel (c): asymptotic time-averaged transport velocity versus the spiking rate λ for three amplitude densities as depicted in panel (a) and for an overall white shot noise intensity $D_P = 10^{-3}$. The remaining parameters are as those given in figure 3 and the thermal fluctuation intensity $D_G = 0.001$.

constant deterministic bias and the mean value of the shot noise $\langle \eta(t) \rangle$ for the case of (i) a moderate spiking rate $\lambda = 4$ and (ii) a large spiking rate $\lambda = 512$. For the low firing rate, one can observe normal transport; for moderate values of the spiking rate λ , we detect small windows of occurrence of ANM. Seemingly, the case with the deterministic bias is most effective for ANM, yielding a wide regime of bias values f . For a large spiking rate of the white shot noise, we do indeed detect convergence towards the deterministic constant bias case; cf. panel (b) in figure 6.

4. Conclusions

With this work we presented a detailed study of the transport properties of an inertial Brownian particle which moves in a periodic, symmetric potential and which in addition is exposed to periodic harmonic ac driving and (generalized) Poissonian white shot noise of finite bias F . We have demonstrated the possibility of manipulating the *direction*

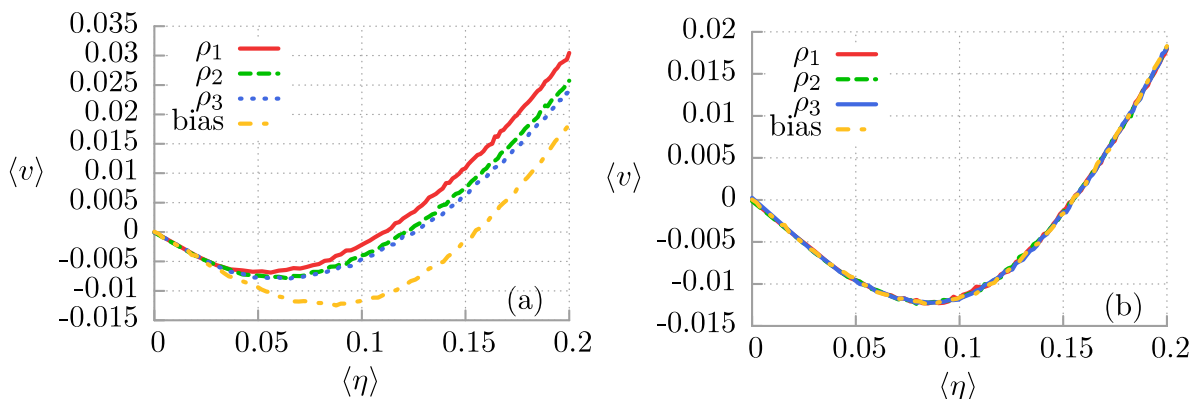


Figure 6. The dependence of the asymptotic time-averaged velocity $\langle v \rangle$ on the constant bias f versus the asymptotic time-averaged mean value of the shot noise $\langle \eta(t) \rangle$ for $\lambda = 4$ in panel (a) and $\lambda = 512$ in panel (b). The thermal fluctuation intensity is $D_G = 0.001$. The remaining parameters are the same as in panel (b) of figure 2. Perfect equivalence (i.e. indistinguishable line plots) of the deterministic and random forcing is observed for a high spiking rate of δ -pulses of Poissonian noise .

of transport just by adjusting the parameters of the white shot noise. Moreover, in such systems, Poissonian white shot noise can induce anomalous transport effects. In particular, such dynamics is able to exhibit an absolute negative mobility regime. This ANM phenomenon has its roots in a purely stochastic dynamics of the system and is robust with respect to the distribution of the random amplitudes of the δ -pulses. In some regions of parameter space, one can find an impact of Poissonian shot noise similar to that of the deterministic bias. In general, the exact equivalence of the two sources of bias does not hold true. However, in the ANM regime the equivalence is observed in the limiting case of a spiking rate $\lambda \rightarrow \infty$ of the δ -pulses. For moderate to large λ , the ANM induced by shot noise is suppressed as compared with the case for a deterministic bias. Notably, for a small spiking rate λ , the ANM response is no longer present and instead a normal, Ohmic-like behavior occurs.

Our results can readily be experimentally tested with an accessible setup consisting of a single resistively and capacitively shunted Josephson junction device operating in its classical regime.

Acknowledgments

This work was supported in part by the grant N202 052940 (JS and JL) and the ESF Program ‘Exploring the Physics of Small Devices’ (PH and JL).

References

- [1] Höpfel R A, Shah J, Wolff P A and Gossard A C, 1986 *Phys. Rev. Lett.* **56** 2736
- [2] Keay B J, Zeuner S, Allen S J, Maranowski K D, Gossard A C, Bhattacharya U and Rodwell M J W, 1995 *Phys. Rev. Lett.* **75** 4102
Zeuner S *et al*, 1996 *Phys. Rev. B* **53** R1717

- Cannon E H, Kusmartsev F V, Alekseev K N and Campbell D K, 2000 *Phys. Rev. Lett.* **85** 1302
- [3] Warman J M, Sowada U and De Haas M P, 1985 *Phys. Rev. A* **31** 1974
Suvakov M, Ristivojevic Z, Petrovic Z Lj, Dujko S, Raspopovic Z M, Dyatko N A and Napartovich A P, 2005 *IEEE Trans. Plasma Sci.* **33** 532
- [4] van der Zant H S J, Slot E, Zaitsev-Zotov S V and Artemenko S N, 2001 *Phys. Rev. Lett.* **87** 126401
- [5] Ros A, Eichhorn R, Regtmeier J, Duong T T, Reimann P and Anselmetti D, 2005 *Nature* **436** 928
Eichhorn R, Regtmeier J, Anselmetti D and Reimann P, 2010 *Soft Matter*. **6** 1858
- [6] Kaya I I and Eberl K, 2007 *Phys Rev. Lett.* **98** 186801
- [7] Xu X B *et al.*, 2007 *Phys. Rev. B* **75** 224507
- [8] Nagel J, Speer D, Gaber T, Sterck A, Eichhorn R, Reimann P, Ilin K, Siegel M, Koelle D and Kleiner R, 2008 *Phys. Rev. Lett.* **100** 217001
- [9] Salger T, Kling S, Denisov S, Ponomarev A V, Hänggi P and Weitz M, 2012 arXiv:1202.5174
- [10] Hartmann L, Grifoni M and Hänggi P, 1997 *Europhys. Lett.* **38** 497
- [11] Reimann P, Kawai R, Van den Broeck C and Hänggi P, 1999 *Europhys. Lett.* **45** 545
Van den Broeck C, Bena I, Reimann P and Lehmann J, 2000 *Ann. Phys.* **9** 713
- [12] Eichhorn R, Reimann P and Hänggi P, 2002 *Phys. Rev. Lett.* **88** 190601
- [13] Eichhorn R, Reimann P and Hänggi P, 2002 *Phys. Rev. E*. **66** 066132
- [14] Cleuren B and Van den Broeck C, 2002 *Phys. Rev. E* **65** 030101(R)
Haljas A, Mankin R, Sauga A and Reiter E, 2004 *Phys. Rev. E* **70** 041107
- [15] Machura L, Kostur M, Talkner P, Luczka J and Hänggi P, 2007 *Phys. Rev. Lett.* **98** 040601
- [16] Machura L, Kostur M, Talkner P, Hänggi P and Luczka J, 2008 *Phys. Rev. B* **77** 104509
Machura L, Kostur M, Talkner P, Hänggi P and Luczka J, 2010 *Physica E* **42** 590
- [17] Machura L, Kostur M, Luczka J, Talkner P and Hänggi P, 2008 *Acta Phys. Pol. B* **39** 1115
- [18] Speer D, Eichhorn R and Reimann P, 2007 *Phys. Rev. E* **76** 051110
- [19] Hennig D, 2009 *Phys. Rev. E* **79** 041114
Du L-C and Mei D-C, 2011 *J. Stat. Mech.* **P11016**
- [20] Hänggi P, Marchesoni F, Savel'ev S and Schmid G, 2010 *Phys. Rev. E* **82** 041121
- [21] Januszewski M and Luczka J, 2011 *Phys. Rev. E* **83** 051117
- [22] Hänggi P and Marchesoni F, 2009 *Rev. Mod. Phys.* **81** 387
Astumian R D and Hänggi P, 2002 *Phys. Today* **55** 33
- [23] Hänggi P, 1978 *Z. Phys. B* **30** 85
- [24] Jung P and Hänggi P, 1990 *Phys. Rev. A* **41** 2977
Jung P and Hänggi P, 1991 *Phys. Rev. A* **44** 8032
Gammaitoni L, Hänggi P, Jung P and Marchesoni F, 1998 *Rev. Mod. Phys.* **70** 223
- [25] Hänggi P, 1980 *Z. Phys. B* **36** 271
Hänggi P, 1981 *Z. Phys. B* **43** 269
- [26] Luczka J, 1999 *Physica A* **274** 200
Machura L, Kostur M and Luczka J, 2008 *BioSystems* **94** 253
- [27] Jung P, Kissner J G and Hänggi P, 1996 *Phys. Rev. Lett.* **76** 3436
Mateos J L, 2000 *Phys. Rev. Lett.* **84** 258
- [28] Hänggi P, Talkner P and Borkovec M, 1990 *Rev. Mod. Phys.* **62** 251
- [29] Kautz R L, 1996 *Rep. Prog. Phys.* **59** 935
- [30] Coffey W T, Kalmykov Yu P and Waldron J T, 2004 *The Langevin Equation* (Singapore: World Scientific)
- [31] Fulde P, Pietronero L, Schneider W R and Strässler S, 1975 *Phys. Rev. Lett.* **35** 1776
Dieterich W, Peschel I and Schneider W R, 1977 *Z. Phys. B* **27** 177
Geisel T, 1979 *Solid State Commun.* **32** 739
- [32] Grüner G, Zawadowski A and Chaikin P M, 1981 *Phys. Rev. Lett.* **46** 511
- [33] Kim C, Lee E, Hänggi P and Talkner P, 2007 *Phys. Rev. E* **76** 011109
- [34] Grigoriu M, 2009 *Phys. Rev. E* **80** 026704
- [35] Januszewski M and Kostur M, 2010 *Comput. Phys. Commun.* **181** 183
- [36] Hänggi P, Bartussek R, Talkner P and Luczka J, 1996 *Europhys. Lett.* **35** 315
Luczka J, Bartussek R and Hänggi P, 1995 *Europhys. Lett.* **31** 431